JOURNAL OF SOLID STATE CHEMISTRY 118, 254–260 (1995)

Solvent Influence on Kinetics and Dissolution Mechanism of Quartz in Concentrated Basic Media (NaOH, KOH, LiOH)

M. Deleuze, A. Goiffon, A. Ibanez, and E. Philippot[1]

Laboratoire de Physicochimie des Matériaux Solides LPMS, URAD0407 CNRS, Place E. Bataillon-case 003, 34095 Montpellier Cedex 5, France

Received October 26, 1994; in revised form February 6, 1995; accepted March 23, 1995

Quartz chemical lapping of AT and SC cuts in concentrated basic solvents and mixtures (NaOH, KOH, LiOH) has led us to study the dissolution mechanism of quartz in order to explain the experimental results in terms of kinetic evolutions. Using X-ray diffraction and ^{29}Si NMR analysis of the species in solution, we propose a dissolution mechanism of quartz in concentrated basic solutions. According to the dissolution process, and taking into account the nature and the size of the alkali cation of the solvent, we explain the kinetic curve evolution. © 1995 Academic Press, Inc.

I. INTRODUCTION

In previous studies (1–3), based on the reverse thermodynamic relations for growth and dissolution processes, we have investigated the chemical polishing, or controlled dissolution, of AT and SC quartz plates in concentrated basic media, NaOH and KOH. The good results obtained have led to the manufacturing of very good high-frequency piezoelectric devices with AT and SC cuts chemically thinned (even after several hundreds of μm have been removed) (4). It appears that the crystallographic orientations have a great influence on the controlled dissolution process. So, the polishing of AT cuts by a NaOH medium leads to a very good surface state, whereas the SC cuts are well polished by a KOH medium. To find a common solvent for these two cuts, we have tested several mixtures of these media and another similar basic solvent, LiOH (5). The phenomena observed during the dissolution (which are influenced by both the solvents and the crystalline orientation) led us to study the dissolution mechanism of quartz in a concentrated basic medium in order to explain the dissolution rate variations observed with different media.

In previous works, studies on silica and quartz solubilities have been performed under conditions quite different from ours, using either diluted hydroxide solutions or hydrothermal conditions (high temperature and pressure) (6–12). Thus, valuable comparisons are difficult to extrapolate.

On the other hand, with the goal of our investigation being the polishing or "controlled dissolution" of quartz material, we have only investigated the solid/solution interface but not the ionic equilibria within the solution. Moreover, these solutions are highly concentrated in hydroxyl and alkali ions, but not in silicium ones; thus, their investigation would not be easy at all because the *in situ* methods used to specify the present chemical species are rare and difficult to use under our extreme conditions (a high hydroxide concentration in a PTFE vessel).

Thus, in this paper, we propose a chemical dissolution mechanism of quartz in high concentrated basic solvents based on our kinetic results. We also try to explain the influence of the solvents on these kinetics. The influence of the superficial crystal structure of the wafers is discussed elsewhere (13).

II. EXPERIMENTS

The dissolution reactor, thermally insulated and waterproofed, described in previous studies (1, 2) is in PTFE to avoid chemical corrosion. The samples used to measure the dissolution rate are AT- and SC-polished discs of 5 to 8 mm in diameter and about 600 μm in thickness.

The thinning is followed by frequency measurements. Indeed, for piezoelectric plates, the resonance frequency is given by:

$$F\,(\text{MHz}) = \frac{K(\text{MHz} \cdot \mu\text{m})}{e(\mu\text{m})},$$

where e is the plate thickness and K is a constant characteristic of the material and of its orientation. For AT quartz plates, K is equal to 1670 MHz · μm and for SC cuts, K is equal to 1820 MHz · μm (14).

Dissolution baths were prepared from high-purity basic products. The percent is expressed in moles.

[1] To whom correspondence should be addressed.

0022-4596/95 $12.00

The dissolution rate is calculated from frequency measurements:

$$V = \frac{\Delta e}{\Delta t} = \left(\frac{K}{F1} - \frac{K}{F2}\right)/\Delta t,$$

where $F1$ and $F2$ are, respectively, the initial and the final frequencies, K is the frequency constant, and Δt is the dissolution time.

To study the dissolution mechanism of quartz in a concentrated basic medium, we have dissolved a quartz crystal in a known quantity of solvent placed in an autoclave. The autoclave was filled to 20% and the temperature was maintained under the boiling point to avoid increasing the pressure. Thus, the composition of the bath has been analyzed by ^{29}Si NMR and by X-ray diffraction methods in order to identify the silicate species.

III. RESULTS AND DISCUSSION

III.1. Dissolution Kinetics of AT and SC Quartz Plates in Basic Media and Mixtures

We have measured the dissolution rate of AT and SC quartz plates in different basic media: NaOH · xH$_2$O (x = 1, 2), KOH · xH$_2$O (x = 0.48, 1) and in several mixtures: NaOH · H$_2$O + KOH · H$_2$O (50/50) and NaOH · H$_2$O + x% LiOH · H$_2$O (x = 11 or 20%). The dissolution kinetics, plotted in Fig. 1, show that the dissolution rate is strongly influenced by both the temperature and the solvent.

From Fig. 1, we can deduce that:

—Dissolution rates in NaOH · H$_2$O or in NaOH · H$_2$O +KOH · H$_2$O baths are quite equal for AT and SC cuts, whereas they are slightly different in KOH · H$_2$O ($V_{SC} > V_{AT}$) and in the mixture NaOH · H$_2$O + x% LiOH · H$_2$O (x = 11 and 20) ($V_{AT} > V_{SC}$);

—The rate for mixture NaOH · H$_2$O + KOH · H$_2$O (50/50) is situated between those of the two pure solvents. Nevertheless, we observe that it is closer to the rate of NaOH · H$_2$O;

—Kinetics of both AT and SC plates depend on the solvent. This implies that the nature of the solvent influences the dissolution rate. Therefore, it appears that the addition of a small quantity of monohydrated lithium hydroxide in soda strongly increases the dissolution rate in terms of the percent added (Table 1). These results indicate that the cation plays an important role in the evolution of the dissolution rate. Thus, we think that the cation size seems to be the most important parameter in explaining the dissolution rate variations. This effect will be developed in Section III.4.

On the other hand, the dissolution rate is strongly influenced by the temperature. The exponential variation corresponds to a thermically activated mechanism, following Arrhenius's law, $k_T = A \cdot \exp(-E_a/RT)$, where k_T is directly related to the dissolution rate $V = K_T(\text{conc})^\alpha$ (conc is the concentration of all species influencing the dissolution mechanism and α is the reaction order). The activation energy E_a (kJ · mole^{-1}) can be calculated from $\ln(V) = f(1/T)$ with $V = A' \cdot \exp(-E_a/RT)$ (V is the dissolution rate in μm/hr and A' is the preexponential term including the frequency factor A and the solution concentration factor (conc$^\alpha$)). Table 2 summarizes all the activation energies calculated from the kinetic curves.

Because the error in the activation energy determination is 6% with $\Delta T = \pm 1$°C, we can consider that all the E_a values are the same and, thus, the same chemical dissolution process must take place. These values are in total agreement with previous results obtained in diluted basic concentrations (15).

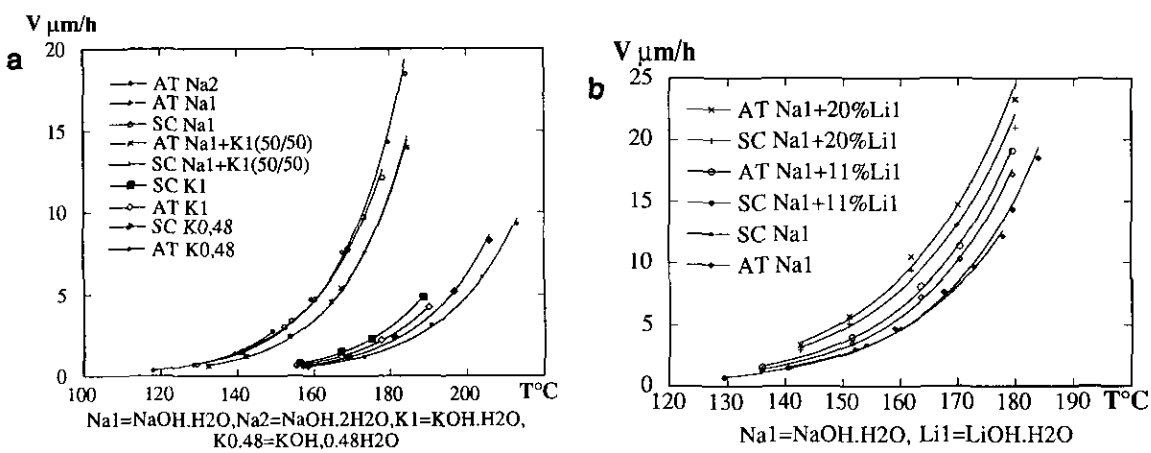

FIG. 1. Dissolution rate plotted against temperature of AT and SC cuts in: (a) NaOH, KOH, and their mixture; (b) NaOH and its mixture with LiOH.

TABLE 1
Increase in Dissolution Rate by Addition of $LiOH \cdot H_2O$ Compared with $NaOH \cdot H_2O$

Temperature	Cut	$NaOH \cdot H_2O$ + 11%$LiOH \cdot H_2O$	$NaOH \cdot H_2O$ + 20%$LiOH \cdot H_2O$
168°C	AT	+34%	+105%
168°C	SC	+25%	+77%
160°C	AT	+35%	+99%
160°C	SC	+21%	+66%

TABLE 2
Activation Energies Calculated for All the Media Used

Solvents	E_a (kJ · mole^{-1}) AT	SC
$NaOH \cdot H_2O$	91	88
$NaOH \cdot 2H_2O$	89	
$KOH \cdot 0.48H_2O$	90	93
$KOH \cdot H_2O$	90	94
$NaOH \cdot H_2O$ + $KOH \cdot H_2O$ (50/50)	91	94
$NaOH \cdot H_2O$ + 11%$LiOH \cdot H_2O$	87	90
$NaOH \cdot H_2O$ + 20%$LiOH \cdot H_2O$	91	91

III.2. ^{29}Si NMR and X-Ray Diffraction Studies of Species in Solution of $NaOH \cdot xH_2O$ (x = 1,2,3) + SiO_2

We have investigated three concentrations $NaOH \cdot xH_2O$ (x = 1, 2, 3). After the quartz dissolution, the liquid mixture (for $NaOH \cdot 2H_2O$ and $NaOH \cdot 3H_2O$) is analyzed using ^{29}Si NMR and the viscous or solid mixture (for $NaOH \cdot H_2O$) is analyzed using X-ray diffraction.

For the presentation of the structure of building units, or silicate anions in the following, the commonly used Q^n notation is adopted (16, 17). In this notation, Q represents a silicon atom bonded to four oxygen atoms forming a tetrahedron. The superscript n indicates the connectivity, i.e., the number of other Q units attached to the SiO_4 tetrahedron under study. Thus Q^0 denotes the monomeric orthosilicate anion SiO_4^{4-}, Q^1 denotes end groups of chains, Q^2 denotes middle groups in chains or cycles, Q^3 denote, chain branching sites, and Q^4 denotes three-dimensionally cross-linked groups. The degree of protonation is ignored in this description. A subscript denotes the number of equal Q^n units in the silicate species in question. A schematic representation and some examples of the Q notation are shown in Table 3.

The ^{29}Si NMR spectra of liquid solutions: $NaOH \cdot 2H_2O + SiO_2$ and $NaOH \cdot 3H_2O + SiO_2$ are shown in Fig. 2. The chemical shift range of the principal groups Q^n is given in Table 4.

The comparison between NMR spectra and chemical shift range of groups allows the identification of the species in solution. It appears that in $NaOH \cdot 3H_2O$ solution, the single signal observed at −71.3 ppm indicates the presence of a Q^0 group corresponding to an orthosilicate SiO_4^{4-} unit. On the other hand, for $NaOH \cdot 2H_2O$ solution, the dissolution of quartz leads to two signals. The first signal at −71.2 ppm corresponds to the monomeric species SiO_4^{4-} (Q^0) and the second signal at −78.2 ppm is attributed to disilicate $Si_2O_7^{6-}$ units. Indeed, if there were silicate chains, other signals corresponding to Q^2 and Na_2SiO_3 should be present. Nevertheless, this *ex situ* ^{29}Si NMR study of equilibrated solutions cannot undoubtedly prove the existence of these SiO_4^{4-} and $Si_2O_7^{6-}$ groups as primary products of the dissolution process.

On the other hand, for the solid $NaOH \cdot H_2O + SiO_2$, the X-ray diffraction pattern shows only the presence of Na_2SiO_3 (Na_4SiO_4 and $Na_6Si_2O_7$ are absent). Table 5 summarizes the results obtained by NMR and X-ray diffraction.

TABLE 3
Notation for Building Units and Silicate Anions (16)

O^- $-O\ Si\ O^-$ O^-	O^- $-O\ Si\ O\ Si$ O^-	O^- $Si\ O\ Si\ O\ Si$ O^-	Si O $Si\ O\ Si\ O\ Si$ O^-	Si O $Si\ OSiO\ Si$ O Si
Q^0 monomer	Q^1 end group	Q^2 middle group	Q^3 branching group	Q^4 cross-linking group
$O^-\ O^-$ $^-O\ Si\ O\ Si\ O^-$ $O^-\ O^-$		$O^-\ O^-\ O^-\ O^-$ $^-O\ Si\ O\ Si\ O\ Si\ O\ Si\ O^-$ $O^-\ O^-\ O^-\ O^-$		$O^-\ O^-$ $^-O\ Si\ O\ Si\ O^-$ $O\quad O$ $^-O\ Si\ O\ Si\ O^-$ $O^-\ O^-$
Q_2^1 dimer		$Q_2^1\ Q_2^2$ linear tetramer		Q_4^4 cyclic tetramer

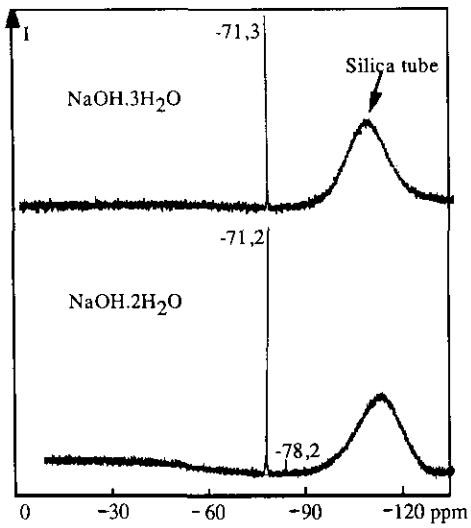

FIG. 2. ^{29}Si NMR spectra of species in solution for SiO_2 + NaOH · xH_2O (x = 2, 3).

III.3. Dissolution Mechanism of Quartz in Concentrated Basic Medium

Identical activation energies and identified species after dissolution allow us to propose a dissolution process of quartz in a concentrated basic medium. Two types of reactions between quartz and soda are given in the literature (24, 25):

The first type of reaction leads to the formation of sodium orthosilicate Na_4SiO_4 and then to $Na_6Si_2O_7$ by the action of water (24):

$$8\ NaOH + 2\ SiO_2 \rightarrow 2\ Na_4SiO_4 + 4\ H_2O \qquad [1]$$

$$2\ Na_4SiO_4 + H_2O \rightarrow Na_6Si_2O_7 + 2\ NaOH. \qquad [1']$$

With the second type of reaction, the sodium metasilicate Na_2SiO_3 is formed (25):

$$SiO_2 + 2\ NaOH \rightarrow Na_2SiO_3 + H_2O. \qquad [2]$$

Knowing that the silicate anion distribution is influenced by the cation-to-Si ratio (16), we can suppose that,

TABLE 4
Chemical Shift of Some Silicate Species (18–23)

Q^n	Chemical shift in ppm/TMS
Monomer Q^0	73.5 to −70
Dimer Q_2^1	−81.1 to −78.3
End group Q^1	−80.7 to −77.5
Middle group Q^2	−90.50 to −86.70
$^-O_3Si\ OSiO_3SiO_3SiO_3^-\ Na_2SiO_3$	−81.2 to −78.8

TABLE 5
Identified Silicate Species after Dissolution of Quartz into Sodium Hydroxide

Analyzed compounds	Silicate species
SiO_2 + NaOH · $3H_2O$	SiO_4^{4-}
SiO_2 + NaOH · $2H_2O$	SiO_4^{4-} and $Si_2O_7^{6-}$
SiO_2 + NaOH · H_2O	$(Si_2O_6)_n^{4n-}$

in more diluted solution (NaOH · $3H_2O$) the solubility of quartz is lower, so that Na/Si ratio is greater and there are only monomer species. In contrast, when the OH^- concentration increases, the solubility of quartz is higher, and the Na/Si ratio decreases and leads to a dimerization of silicate ions.

In Fig. 3, we have represented the proposed mechanism. During the first step, the quartz is dissolved into monomeric species, hydroxide anions react on silicium, and Na^+ cations on oxygen atoms are present in the material. Thus, Si–O–Na groups are created and generate an electron displacement. This phenomenon weakens the surrounding bonds and leads to the breaking of the nearest bonds and to the dissolution by forming SiO_4^{4-} anions.

The second step corresponds to the formation of dimeric species, $Si_2O_7^{6-}$, and the third, to the association in silicate chains, Na_2SiO_3.

In this study, we have only investigated the dissolution mechanism in sodium hydroxide but we think that, for the other solvents, the same mechanism takes place with different cations. This assumption is supported by the equality of the activation energies. In the next section, the influence of the cations themselves will be specified.

III.4. Influence of Solvent Nature on Kinetic Evolutions

Based on the dissolution mechanism described in Section III.3 and on the characteristics of different alkali cations, the difference in the dissolution rate evolution with the nature of the solvent has been explained.

First, we must consider the solvation degree of the ionic species present in solution. In this study, we assume, due to the high concentration, that the cations are not hydrated. This approximation is confirmed by the dissolution rates (Fig. 1) and by the studies of Dove and Crerar (26) concerning the quartz dissolution under pressure with diluted LiCl, NaCl, and KCl solutions. The authors found the smallest dissolution rate for LiCl and attributed this behavior to the high hydration energy of lithium in aqueous solutions, which creates large hydration sphere of strongly oriented water molecules around the lithium ion. This makes the Si–O bonds less available for an attack by lithium. In contrast, in our study, the

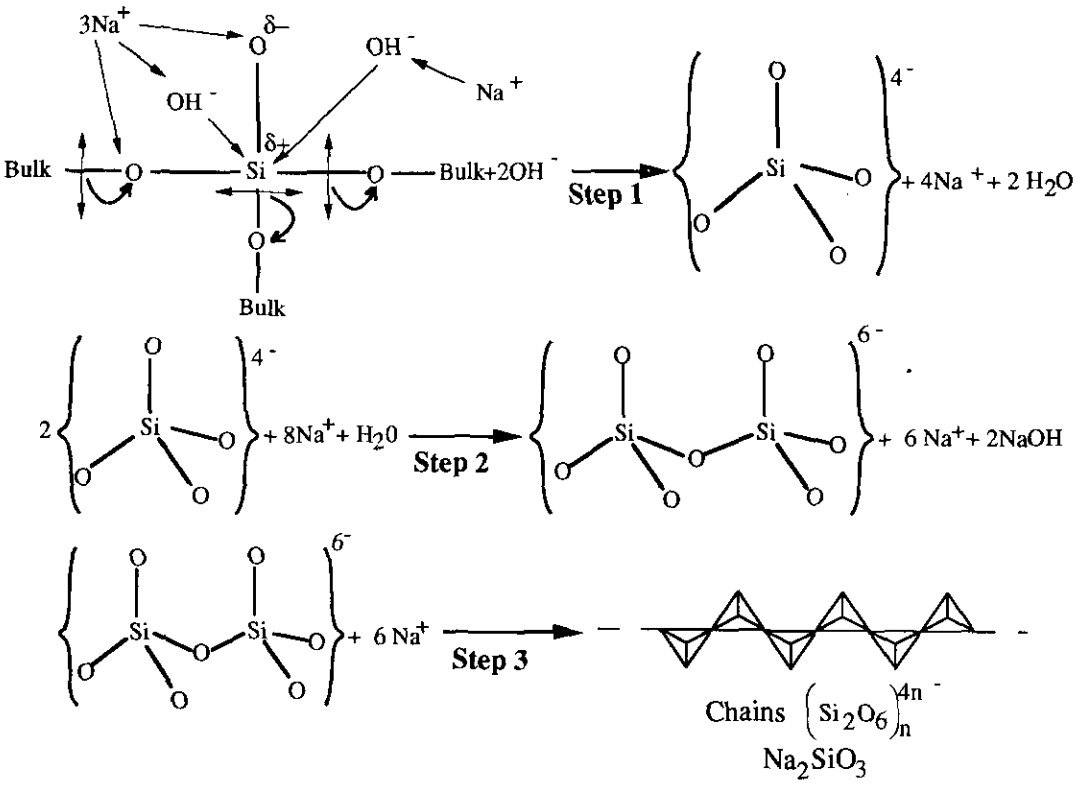

FIG. 3. Dissolution mechanism of quartz in concentrated basic solutions.

addition of $LiOH \cdot H_2O$ generates an increase in the dissolution rate. This result indicates that, as we assume, lithium cations are only slightly or not at all hydrated and it must be the same for the other cations, K^+ and Na^+.

The experimental dissolution rates, plotted in Fig. 1, indicate that the nature of the cation is the most important parameter that explains the difference between solvents, i.e., why $V_{Li^+} > V_{Na^+} > V_{K^+}$. However, it appears that four effects must be taken into account to explain the observed evolution:

—the polarizing power of the cation;
—the size of the cation associated with steric effects;
—the solvent concentration; and
—the atomic surface structure of the plates.

This last parameter has been discussed elsewhere (13).

III.4.1. Polarizing power of the cation. For alkali cations, effective radius (r) increases with atomic number. At the cation surface, which is assumed to be spherical, the nuclear charge generates a field varying with $1/r^2$. Values of effective radii (r) and relative field (H) are presented in Table 6.

According to the approximation of the nonhydrated cation and dissolution mechanism, the dissolution rate evolution can be explained. According to the alkali cation, the displacement of electrons will be most important when the cation is the smallest, i.e., when its relative field (H) is the highest. So, the bond breaking will be easier when the cation size is smaller and, according to the relative field values, $V_{Li^+} > V_{Na^+} > V_{K^+}$, which is in agreement with the observed experimental dissolution rates.

III.4.2. Steric effects due to the cation size. To analyze the steric effect, we have used the *ab initio* calculations of the bond lengths and angles of an alkali cation approaching a H_4SiO_4 molecule (28–30). This model assumes conditions of 0 K and zero pressure to predict the equilibrium configuration of an isolated, nonhydrated molecule. Using this model, the minimum enegy geometrics of the static molecules NaH_3SiO_4 and LiH_3SiO_4 are

TABLE 6
Effective Ionic Radius, r, and Relative Field $H \approx f(1/r^2)$ of Li^+, Na^+, K^+ Cations (27)

	Li^+	Na^+	K^+
Effective ionic radius r (Å)	0.59	1.00	1.38
Relative field H	1.00	0.63	0.34

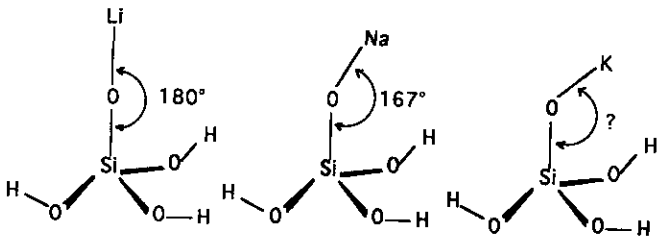

FIG. 4. Optimized bond angles for the static molecular models (*ab initio*) of NaH_3SiO_4 and LiH_3SiO_4 (28). Extrapolation for KH_3SiO_4.

predicted and they are shown in Fig. 4. The KH_3SiO_4 molecule configuration is not calculated, but taking into account the nature of K^+, we think that the Si–O–K angle must be less than the Si–O–Li and Si–O–Na angles.

Assuming that the presence of alkali cation gives to the quartz surface structure a form similar to that shown in Fig. 5, we can compare the weakening of the Si–O–Si linkages using different cations. According to the dissolution mechanism (Fig. 3), on the quartz surface, there is a formation of Si–O–*M* (*M* = Li^+, Na^+, K^+) groups and the more open Si–O–*M* bond angles increase the accessibility of hydroxide ions and other cations to the Si–O bonds. Thus, steric effects due to the Si–O–*M* bond angles allow us to determine the dissolution rate evolution versus the cation size: $V_{Li^+} > V_{Na^+} > V_{K^+}$, in agreement with the experimental results.

III.4.3. Solvent concentration. In Fig. 1a, it can be observed that, in soda, the dissolution rate is basically the same whatever its concentration while, in potassium hydroxide, the dissolution rate slowly increases with the dilution, which is an unexpected result. Previous works (15) on quartz dissolution in diluted basic media had concluded that the dissolution rate varied as $[OH^-]^{1/2}$ in low concentration and become $[OH^-]$ independent for high alkalinity. This last result is attributed to a quartz surface saturation by OH^-. In our case, considering the very high concentration of the solutions and in view of the fact that the rate-limiting step must be the removal of SiO_4 sites, no rate variation should be observed. To explain our results, it can be assumed that the rate of desorption of SiO_4^{4-} entities is favored by the decrease in the viscosity of the solution, which may be the factor limiting the overall rate of dissolution (31).

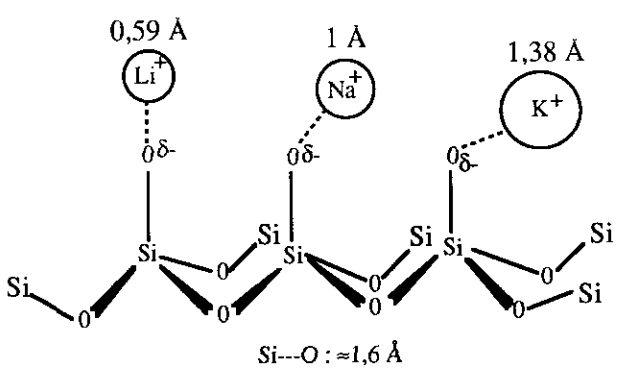

FIG. 5. Schematic representation of adsorbed cations at the quartz surface.

IV. CONCLUSION

We have investigated the dissolution kinetics of AT and SC quartz plates in concentrated basic solvents NaOH, KOH, and their mixtures with LiOH. The activation energies calculated from kinetic curves show that the same dissolution process must take place. According to these results for all the studied solvents, we have proposed a single dissolution mechanism of quartz in concentrated basic solutions: the quartz dissolution is based on the hydroxide ion acting on silicium atoms with the alkali cation interacting with oxygen atoms simultaneously. This double mechanism leads to a weakening of Si–O bonds and SiO_4^{4-} species are formed. Furthermore, differences in the dissolution rate between different solvents can be explained by taking into account the cation size (polarizing power, steric effect) and the dilution factor.

However, as shown in previous studies, the crystallographic orientation has a great influence on the dissolution rate. To explain these variations, we must consider the atomic structure of the crystal surface and introduce a parameter called "dissolution site." Elsewhere we have discussed and tried to explain both the differences in dissolution rates and the differences in polishing properties related to plate orientation and solvent, based on the crystallographic structure and the nature of the solvents (13).

ACKNOWLEDGMENTS

The authors thank Thomson/CEPE and CNRS for their financial support.

REFERENCES

1. M. Deleuze, A. Goiffon, A. Ibanez, and E. Philippot, *in* "Proceedings, 7th European Frequency and Time Forum" p. 255, 1993.
2. M. Deleuze, O. Cambon, A. Goiffon, A. Ibanez, and E. Philippot, *J. Mater. Sci.* **29**, 5390 (1994).
3. M. Deleuze, O. Cambon, A. Goiffon, A. Ibanez, and E. Philippot, *J. Phys.* **4**, 79 (1994).
4. E. Philippot, O. Cambon, A. Goiffon, A. Ibanez, and D. Cachau, France Patent 91.09170.
5. M. Deleuze, A. Goiffon, A. Ibanez, and E. Philippot, submitted for publication.

6. J. A. Van Lier, P. L. De Bruyn, and J. T. G. Overbeek, *J. Phys. Chem.* **64,** 1675 (1960).
7. S. A. Greenberg, and E. W. Price, *J. Phys. Chem.* **61,** 1539 (1957).
8. S. A. Greenberg, *J. Phys. Chem.* **61,** 960 (1957).
9. J. Schwartzentruber, W. Fürst, and H. Renon, *Geochim. Cosmochim. Acta* **51,** 1867 (1987).
10. K. G. Knauss and T. J. Wolery, *Geochim. Cosmochim. Acta* **52,** 43 (1988).
11. J. V. Walther and H. C. Helgeson, *Am. J. Sci.* **277,** 1315 (1977).
12. D. A. Crerar and G. M. Anderson, *Chem. Geol.* **8,** 107 (1971).
13. M. Deleuze, Ph. D. thesis, Montpellier, France, 1994.
14. V. E. Bottom, "Introduction to Quartz Crystal Unit Design," Van Nostrand–Reinhold, New York, 1960.
15. A. J. Gratz, P. Bird, and G. B. Quiro, *Geochim. Cosmochim. Acta* **54,** 2911 (1990).
16. G. Engelhardt, and D. Michel, "High-Resolution Solid-State NMR of Silicates and Zeolites," Wiley, Chichester, 1987.
17. G. Engelhardt, H. Jancke, D. Hoebbel, and W. Wieker, *Z. Chem.* **14,** 109 (1974).
18. G. Engelhardt, D. Zeigan, H. Jancke, D. Hoebbel, and W. Wieker, *Z. Anorg. Allg. Chem.* **17,** 418 (1975).
19. G. Engelhardt, W. Altenburg, D. Hoebbel, and W. Wieker, *Z. Anorg. Allg. Chem.* **43,** 428 (1977).
20. G. Engelhardt, H. Jancke, M. Mägi, T. Pehk, and E. Lippma, *J. Organomet. Chem.* **28,** 293 (1971).
21. R. O. Gould, B. M. Lowe, and N. A. Macgilp, *J. Chem. Soc. Chem. Commun.*, 720 (1974).
22. D. Hoebbel, G. Garzo, G. Engelhardt, and A. Till, *Z. Anorg. Allg. Chem.* **5,** 450 (1979).
23. R. K. Harris, and R. M. Newman, *J. Chem. Soc. Faraday Trans. 2* **73,** 1204 (1977).
24. D'Ans and Löffer, *Chem. Ber.* **63,** 1446 (1930).
25. M. Guerin, "Chimie," Vol. II, Chap. III, Dunod, Paris, 1969.
26. P. M. Dove, and D. A. Crerar, *Geochim. Cosmochim. Acta* **54,** 955 (1990).
27. R. D. Shannon, and C. T. Prewitt, *Acta Crystallogr Sect. B* **25,** 925 (1969).
28. G. V. Gibbs P. D'Arco, and M. B. Boisen, *J. Phys. Chem.* **91,** 5347 (1987).
29. G. V. Gibbs, *Am. Mineral.* **67,** 421 (1982).
30. A. C. Lasaga and G. V. Gibbs, *Am. J. Sci.* **290,** 263 (1990).
31. R. K. Iler, "The Chemistry of Silica," p. 65. Wiley, Chichester, 1987.